

Universal relations for differentially rotating relativistic stars at the threshold to collapse

Gabriele Bozzola¹, Nikolaos Stergioulas², Andreas Bauswein³

¹*Department of Physics, Università degli Studi di Milano, IT-20133 Milano, Italy*

²*Department of Physics, Aristotle University of Thessaloniki, GR-54124 Thessaloniki, Greece*

³*Heidelberg Institute for Theoretical Studies, D-69118 Heidelberg, Germany*

11 September 2017

ABSTRACT

A binary neutron star merger produces a rapidly and differentially rotating compact remnant whose lifespan heavily affects the electromagnetic and gravitational emissions. Its stability depends on both the equation of state (EOS) and the rotation law and it is usually investigated through numerical simulations. Nevertheless, by means of a sufficient criterion for secular instability, equilibrium sequences can be used as a computational inexpensive way to estimate the onset of dynamical instability, which, in general, is close to the secular one. This method works well for uniform rotation and relies on the location of turning points: stellar models that are stationary points in a sequence of equilibrium solutions with constant rest mass or angular momentum. Here, we investigate differentially rotating models (using a large number of equations of state and different rotation laws) and find that several universal relations between properly scaled gravitational mass, rest mass and angular momentum of the turning-point models that are valid for uniform rotation, are insensitive to the degree of differential rotation, to high accuracy.

Key words: relativity – equations of state – methods: numerical – stars: neutron – stars: rotation

1 INTRODUCTION

Neutron stars, the most dense stars known in the Universe, are unique environments to explore physics in a regime so extreme that cannot yet be reproduced in laboratories. Studies on those compact objects have resulted in a deeper understanding of several areas of physics and further advances are expected with the direct detection and analysis of the gravitational waves and electromagnetic signals emitted by coalescing binaries. These systems, formed by two neutron stars orbiting each other and eventually merging, are promising sources for the second generation of gravitational-waves detectors (Accadia et al. 2011; Abadie et al. 2010; Somiya 2012). One can distinguish two different outcomes of mergers depending on the binary mass (Shibata 2005; Shibata & Taniguchi 2006; Baiotti et al. 2008; Hotokezaka et al. 2011; Bauswein et al. 2013). (1) For binary masses below some threshold mass the merger results in the formation of a hot, massive and rapidly spinning neutron star accompanied by a strong emission of gravitational waves. The remnant may eventually collapse at a later time as a result of angular momentum redistribution and energy losses by means of mass ejection, neutrino and gravitational wave emission.

This scenario is referred to as *delayed collapse*¹. (2) For binary masses larger than the threshold mass the remnant is too massive to be stabilized against gravitational collapse and directly forms a black hole on a dynamical timescale. This scenario is known as *prompt collapse*. The stability of the remnant against gravitational collapse (prompt versus delayed collapse) affects the gravitational, neutrino and electromagnetic emission and is thus crucial for multi-messenger observations of binary neutron star mergers (see e.g. Faber & Rasio 2012; Paschalidis & Stergioulas 2016; Baiotti & Rezzolla 2017, for reviews).

In general, the stability of compact stars is determined by the mass, rotation (angular momentum and rotation law), the EOS and the temperature. In the context of binary mergers, numerical simulations show that merger remnants initially have a complex, non-uniform velocity profile and can support masses which exceed the maximum mass of uniformly rotating stars in hydrostatic equilibrium (Shibata et al. 2005; Baiotti et al. 2008; Hotokezaka et al. 2011; Bauswein et al. 2013; Kastaun et al. 2016; Hanauske et al. 2017). Therefore, merger remnants are often modeled and

¹ Note that within this classification the delayed collapse scenario also subsumes cases where the remnant actually remains stable.

described by differentially rotating stars, which can support significantly larger masses than uniformly spinning stellar configurations (see e.g. Baumgarte et al. 2000; Lyford et al. 2003; Morrison et al. 2004; Kaplan et al. 2014; Gondek-Rosińska et al. 2017; Bauswein & Stergioulas 2017). Compact objects with masses exceeding the maximum mass of uniformly rotating stars are usually referred to as *hypermassive neutron stars* (HMNS).

Within this work we investigate rotating stellar equilibrium models with uniform and differential rotation laws. A key tool for studying the stability of uniformly rotating models of relativistic stars is the turning-point method by Friedman, Ipser and Sorkin (Friedman et al. 1988) for equilibrium sequences. A uniformly rotating equilibrium stellar model will have central energy density ϵ_c , gravitational mass M , rest mass M_0 and angular momentum J . An *equilibrium sequence* is a one-dimensional slice indexed by some parameters of the whole space of equilibrium models. The sequences we studied in this work are constructed by varying the central energy density ϵ_c and holding fixed one of the other quantities. In this case, a *turning point* in a sequence occurs when two out of three first derivatives with respect to ϵ_c vanish. For example, in a sequence of constant angular momentum J by construction $\partial J/\partial \epsilon_c = 0$, therefore a turning point is a stationary point of the function $M = M(\epsilon_c)$. The Friedman, Ipser and Sorkin criterion implies that for equilibrium sequences of uniformly rotating stars at a turning point:

- (i) the derivative of the third quantity also vanishes,
- (ii) the sequence becomes secularly unstable.

The theorem is based on the assumption that the variation of the total energy depends only on the change in rest mass and angular momentum, and not in their redistribution (which would correspond to a second derivative). This assumption is justified by the fact that the second effect has a longer timescale. Moreover, the criterion holds also for hot stars with the only difference that the triplet (M_0, M, J) has to be enlarged to include entropy S and thus it is required that three first derivatives out of four vanish Kaplan et al. (2014). For cold stars, however, entropy is not relevant to the stability because a change in entropy does not produce a variation in energy. In this case, point (i) of the theorem implies that the stationary point of the sequences with J fixed must coincide with the ones of the sequences with M_0 fixed. Point (ii), on the other hand, implies that the criterion is only a sufficient: it does not state that all unstable models are located on one side of a turning point, but it guarantees that every model on that side is unstable. Even if point (ii) posits that the turning-point line marks the onset of secular instability, there are reasons to assume that also the dynamical-instability line has to be close (Takami et al. 2011; Friedman & Stergioulas 2013; Kaplan et al. 2014). Indeed, as angular momentum is redistributed on secular timescales the star encounters the onset of dynamical instability and collapses to a black hole. Thus, the onset of the secular instability separates stable neutron stars from collapsing ones.

The criterion is routinely used to estimate dynamical instability for cold neutron stars (e.g. Takami et al. 2011; Kaplan et al. 2014) and justifies our interest in studying equilibrium sequences.

The Friedman, Ipser and Sorkin's criterion is analyt-

ically proved only for uniformly rotating stars, but it has been found numerically (Kaplan et al. 2014) that even for differentially rotating ones the turning points are indicators of the onset of instability with some accuracy. Despite being not as accurate as complete numerical simulations, this method has the advantage of being computationally less expensive, and thus a large number of stellar models with different EOSs can be constructed and tested.

In this paper we focus our attention on the properties of differentially rotating models for turning-point sequences (i.e. at the threshold of collapse) of constant angular momentum or constant rest mass with varying central energy density. We find that such models satisfy universal relations, which are (to high accuracy) independent of the choice of the EOS and on the details of the rotation law. These relations involve gravitational mass, rest mass and angular momentum rescaled by a proper factor that fixes the physical scale of the system and that is provided by the turning point for the nonrotating sequence. This extends recent work on uniformly rotating stars (Breu & Rezzolla 2016; Lenka et al. 2017) to the case of differential rotation.

The organization of the paper is as follows. Section 2 describes the theoretical and numerical framework used, Section 3 collects our results and presents the universal relations and our application to the threshold mass of binary neutron star mergers. Finally, a summary is left for Section 4. If not stated otherwise, we use geometrized units with $c = G = M_\odot = 1$, where c is the speed of light in vacuum and G the gravitational constant.

2 SETUP AND NUMERICAL METHOD

2.1 Assumptions

We work in full general relativity assuming a stationary and axisymmetric spacetime with coordinates (x^μ) , metric tensor $g_{\mu\nu}$ and line element given by

$$ds^2 = -e^{2\gamma+\rho} dt^2 + e^{\gamma-\rho} (d\phi - \omega dt)^2 + e^{2\alpha} (dr^2 + r^2 d\theta^2), \quad (1)$$

where t, r, θ, ϕ are the *quasi-isotropic coordinates* and $\gamma, \rho, \alpha, \omega$ are four metric functions that depend on the coordinates r, θ only (Bardeen & Wagoner 1971; Friedman & Stergioulas 2013). An equilibrium configuration is found by solving Einstein's field equations

$$\mathcal{R}_{\mu\nu} - \frac{1}{2} g_{\mu\nu} \mathcal{R} = 8\pi T_{\mu\nu}, \quad (2)$$

where $\mathcal{R}_{\mu\nu}$ is the Ricci tensor, \mathcal{R} the Ricci scalar and $T_{\mu\nu}$ the stress-energy tensor of the matter. To model the matter of a neutron star we assume its interior to be a perfect fluid with stress-energy tensor

$$T^{\mu\nu} := (\epsilon + P) u^\mu u^\nu + P g^{\mu\nu}, \quad (3)$$

where ϵ is the energy density, P the pressure and u^μ the four-velocity. In addition, we consider our neutron stars to be cold and we ignore thermal effects. This is because for the temperature expected for merger remnants thermal effects have only a secondary effect on the stability of the remnant, the dominant effect being the stabilisation through differential rotation (see, e.g. Kaplan et al. (2014)).

We assume the star to be rotating with no meridional

currents. Then, the first integral of the hydrostationary equilibrium equation involves the function $F(\Omega) := u^t u_\phi$, where $\Omega := u^\phi / u^t$ is the angular velocity inside the star, with respect to a nonrotating observer at infinity. The choice of this function fixes the rotation law. Here, we study three different rotation laws: *uniform* rotation, the *one-parameter* rotation law by Komatsu et al. (1989a,b), and the *three-parameter* rotation law by Bauswein & Stergioulas (2017).

2.1.1 TOV solution

A special case of equilibrium sequence is the one of non-rotating models with $J = 0$, the so-called TOV solutions (Tolman 1934; Oppenheimer & Volkoff 1939). We introduce for later convenience a shorthand notation for the values of some physical quantities of the nonrotating model with *maximum mass*, which is the turning point of this sequence:

$$M^* := M_{\max}^{\text{TOV}} \quad M_0^* := M_{0, \max}^{\text{TOV}} \quad R^* := R_{\max}^{\text{TOV}}. \quad (4)$$

We also define the maximum compactness as the ratio M^*/R^* . For every rotation law, the maximum-mass TOV model is the end-point of the quasi-radial instability sequence in the limit of zero angular momentum.

2.1.2 Uniform rotation law

The most simple non-trivial rotation law is uniform rotation, where the whole star spins as a rigid body about its axis. This is a good approximation to study old neutron stars. Indeed, angular momentum redistribution, magnetic braking and shear viscosity have the effect of driving the angular velocity profile towards uniform rotation. The assumption of uniform rotation is not accurate when applied to nascent neutron stars or to binary neutron star merger remnants, where differential rotation modifies their bulk properties. Uniform rotation can increase the maximum allowed mass by up to $\sim 25\%$ (Friedman & Ipser 1987). Equilibrium configurations with rest mass larger than M_0^* are called *supramassive*, since they reach the threshold to black hole collapse (rather than the TOV sequence) when spun down.

2.1.3 One-parameter rotation law

The most investigated rotation law is the *one-parameter* law, introduced in Komatsu et al. (1989a,b). This differential rotation is defined by:

$$F(\Omega) := A^2(\Omega_c - \Omega) = \frac{(\Omega - \omega)r^2 \sin^2 \theta e^{-2\rho}}{1 - (\Omega - \omega)^2 r^2 \sin^2 \theta e^{-2\rho}}, \quad (5)$$

where Ω_c is the angular velocity on the axis of rotation. The parameter A has the units of length: it is the length-scale over which the angular velocity varies. Thus, for $A \rightarrow +\infty$ uniform rotation is recovered. A dimensionless parameter is defined as:

$$\hat{A} = \frac{A}{r_e}, \quad (6)$$

where r_e is the coordinate radius at the equator. From a mathematical point of view, the one-parameter law is well-defined for every $\hat{A} \geq 0$, but there are physical reasons to

consider additional constraints on the range of allowed values. A very small value of \hat{A} would describe a star in which a small region near the axis would spin very fast, with the remaining star rotating slowly. For this reason, we consider only models with $\hat{A} > 0.5$ as being astrophysically relevant. Equilibrium models that rotate with this rotation law can support about 50% more mass than the maximum mass non-rotating model (Baumgarte et al. 2000; Lyford et al. 2003; Morrison et al. 2004; Gondek-Rosińska et al. 2017). The term *hypermassive neutron star* is used to refer to a star that has more mass than the maximum allowed for uniformly rotating supramassive stars.

2.1.4 Three-parameter rotation law

The third rotation law we consider is the *three-parameter* law introduced in Bauswein & Stergioulas (2017). This is specified by:

$$\begin{cases} F(\Omega) = A_1^2(\Omega_c - \Omega) + (A_2^2 - A_1^2)(1 - \beta)\Omega_c, & \text{if } \Omega \leq \beta\Omega_c, \\ F(\Omega) = A_2^2(\Omega_c - \Omega), & \text{if } \beta\Omega_c \leq \Omega \leq \Omega_c, \end{cases} \quad (7)$$

which is practically a piecewise extension of the one-parameter law (5) to two different regions inside the star. The regions are separated by the value $\Omega = \beta\Omega_c$. For angular velocities larger than this, the rotation law coincides with (5), with parameter $A = A_2$, and for smaller angular velocities it coincides with (5) (up to a constant), with $A = A_1$. The constant is fixed to ensure continuity of $F(\Omega)$ at the transition $\Omega = \beta\Omega_c$. Moreover, if $\beta = 1$, or if $A_1 = A_2$, the rotation law (7) reduces to the usual one-parameter law (5). The three-parameter rotation law allows for an astrophysically relevant core to have a slower rotating envelope. In this way, higher values of mass are allowed before encountering the mass-shedding limit.

2.1.5 Numerical setup

We use a recent version of the RNS code (Stergioulas & Friedman 1995), which has been extended to include models with the one-parameter rotation law (5) (see Stergioulas et al. 2004) and with the three-parameter rotation law (7) (see Bauswein & Stergioulas 2017). A specific equilibrium model is constructed by choosing the EOS and the rotation law and specifying the central energy density ϵ_c and the ratio of the polar coordinate radius to equatorial coordinate radius, r_p/r_e . Sequences of models with desired properties (such as a given rest mass or angular momentum) can be constructed through an iterative procedure. We set up RNS to use a grid of DMDIV = 251 and DSDIV = 501 (angular times radial grid points) and to reach an internal accuracy of 10^{-7} and a tolerance in the desired value of the parameters of 10^{-4} (see Nozawa et al. 1998; Friedman & Stergioulas 2013, for more information on RNS).

2.2 Equations of state

We consider thirteen cold tabulated EOSs in neutrino-less β -equilibrium, which are all compatible with the observational requirement of a stable, nonrotating neutron star of

mass $2 M_{\odot}$ (Demorest et al. 2010; Antoniadis et al. 2013). Acronyms and references for the EOSs are listed in Table 1, whereas Figure 1 shows the $M = M(R)$ relation for each EOS. In addition, we use a strange star EOS and two polytropic EOSs (for details, see below).

Ten of the thirteen EOSs are obtained by extracting the zero-temperature limit from the tables provided by Hempel (2017), where they are available with full temperature and composition dependence. We impose neutrino-less β -equilibrium, and therefore we choose the value of the lepton fraction such that

$$\mu_p + \mu_e = \mu_n + \mu_{\nu} \text{ with } \mu_{\nu} = 0, \quad (8)$$

where $\mu_{\nu}, \mu_e, \mu_n, \mu_p$ are the chemical potentials for electron neutrinos, electrons, neutrons and protons. The other three zero-temperature, tabulated EOSs (WFF1, WFF2 and MDI) are provided in the distribution of the public domain version of RNS (Stergioulas 1999). Together, these thirteen tabulated EOS cover the currently allowed mass-radius parameter space for nonrotating models well, including very soft, very stiff and several intermediate EOS, as well as an EOS with a large softening due to a phase transition to hyperons, see Figure 1.

The strange star EOS we consider is described by the MIT-bag model of quark matter, with an EOS

$$P(\epsilon) = a(\epsilon - \epsilon_0), \quad (9)$$

see, e.g. Witten (1984); Haensel et al. (1986); Alcock et al. (1986); Zdunik (2000). The parameter ϵ_0 , related to the bag constant, has a value of $\epsilon_0 = 4.2785 \times 10^{14} \text{ g cm}^{-3}$. The value of a is a model-dependent constant which, assuming massless strange quarks, takes the exact value $a = 1/3$. We fixed the surface of the star at the energy density of $4.798 \times 10^{14} \text{ g cm}^{-3}$ (number density 0.28665 fm^{-3}). The $M(R)$ relation for nonrotating strange stars with this EOS is substantially different than for the microphysically motivated tabulated EOSs and it is marginally compatible with observational constraints.

Finally, we consider polytropic EOSs in the form

$$P(\rho) = K\rho^{1+\frac{1}{n}}, \quad (10)$$

where ρ is the rest mass density and K and n are respectively the *polytropic constant* and the *polytropic index*. We included polytropes with index $n = 0.5$ and $n = 1.0$, and we fixed the value of $K = 1$, which corresponds to using the polytropic units as in Cook et al. (1994). The polytropic EOS with $n = 1.0$ mimics roughly an intermediate EOS, whereas the one with $n = 0.5$ yields models that are essentially a stiff core.

2.3 Equilibrium sequences and turning points

We used RNS to construct a mesh of 500 different rotating equilibrium models for each EOS, covering the range of central energy densities $\epsilon_c \in (0.5 \times 10^{15} \text{ g cm}^{-3}, 5 \times 10^{15} \text{ g cm}^{-3})$ with every EOS in Table 1. For polytropes, we used the range $\epsilon_c \in (0.3, 3.0)$ for $n = 0.5$ and $\epsilon_c \in (0.1, 1.0)$ for $n = 1.0$ (in polytropic units). With RNS we could construct models that are either limited by the mass-shedding limit, or that have a small axis ratio down to ~ 0.3 , below which other branches of solutions

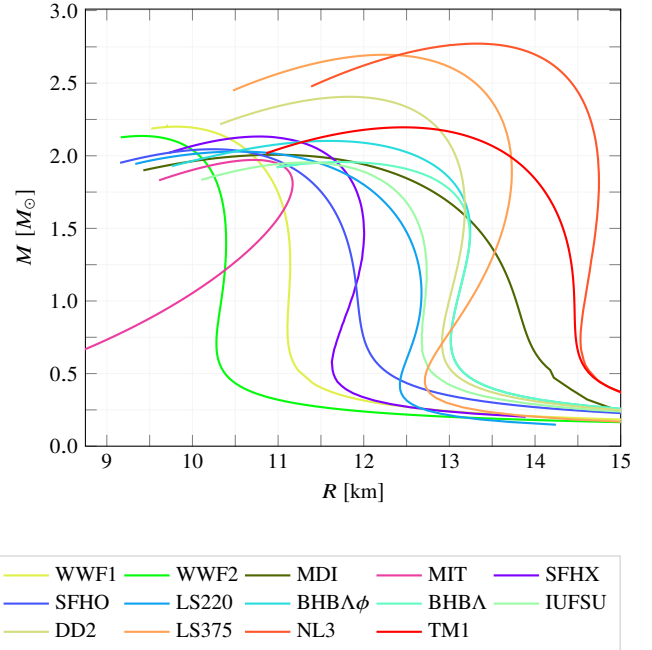


Figure 1. Gravitational mass and radius relation for non-rotating stars with all the tabulated EOSs shown in Table 1. All EOSs produce stellar models that are compatible with the observational mass limit of $2 M_{\odot}$ (Demorest et al. 2010; Antoniadis et al. 2013).

Table 1. Equations of state with references used in this study.

EOS	References
DD2	Hempel & Schaffner-Bielich (2010); Typel et al. (2010)
LS220	Lattimer & Swesty (1991)
LS375	Lattimer & Swesty (1991)
NL3	Lalazissis et al. (1997); Hempel & Schaffner-Bielich (2010)
SFHO	Hempel & Schaffner-Bielich (2010); Steiner et al. (2013)
SFHX	Hempel & Schaffner-Bielich (2010); Steiner et al. (2013)
TM1	Sugahara & Toki (1994); Hempel & Schaffner-Bielich (2010)
IUFSU	Roca-Maza & Piekarewicz (2008); Hempel & Schaffner-Bielich (2010)
BHBA	Hempel & Schaffner-Bielich (2010); Banik et al. (2014)
BHBA ϕ	Hempel & Schaffner-Bielich (2010); Banik et al. (2014)
WFF1	Wiringa et al. (1988)
WFF2	Wiringa et al. (1988)
MDI	Arnett & Bowers (1977)

with the same central energy density and axis ratio may exist (see Gondek-Rosińska et al. 2017; Ansorg et al. 2009). Such models with small axis ratio can have an off-center density maximum (Stergioulas et al. 2004). Because binary neutron star merger remnants are quasi-spherical, with axis ratio that is not much smaller than about 0.4 in the core, we did not include quasi-toroidal models in our sample.

We interpolated with tenth-degree polynomials the obtained equilibrium sequences in the region where we ex-

pected the turning points in the constant rest-mass and constant angular momentum sequences. The turning points were then located by imposing the stationary condition on the first derivative of the best-fitting polynomials. We estimate an error of order 0.5% in the central energy density when locating the turning points.

2.4 Validation of the numerical setup

We verified our numerical setup by recovering the well-established result that for uniformly rotating stars the location of the turning points of constant rest mass sequences must coincide with the location of the turning points for constant angular momentum sequences. We computed the turning points for both kinds of sequences for all the EOSs in Table 1 and for the two polytropic EOSs, with uniform rotation. Specifically, for each tabulated EOS we constructed ten sequences with constant angular momentum with $J \in (0.5, 7.0)$ and ten with constant rest mass (the range depended on the EOS). For the polytropic EOS we computed twenty equispaced sequences with parameters (in polytropic units) $J \in (0.5 \times 10^{-4}, 2.5 \times 10^{-2})$ and $M \in (0.15, 0.19)$ for the $n = 0.5$ and $J \in (0.5 \times 10^{-4}, 2.5 \times 10^{-2})$ and $M \in (0.18, 0.22)$ for $n = 1.0$.

As expected, we found that interpolating the turning points for the two kinds of sequences with a fifth-order polynomial the two obtained curves are compatible within a relative error of 0.5% in the central energy density.

3 RESULTS

3.1 Universal relations

3.1.1 One-parameter rotation law

We studied the one-parameter rotation law with two representative cases of a soft EOS (SFHO) and a stiff one (NL3). We sampled the parameter space with ten equispaced values of \hat{A} from $\hat{A} = 0.5$ to $\hat{A} = 2.0$ and with the values $\hat{A} \in \{2.5, 3.0, 4.0\}$. The locations of the turning points with $\hat{A} = 4.0$ are indistinguishable from the uniformly rotating ones within the tolerance of our method. Therefore, we consider that this value recovers uniform rotation with high accuracy and focus on a range of \hat{A} which produce results considerably different than compared to uniform rotation. We computed the turning points for ten equispaced equilibrium sequences of constant angular momentum $J \in (0.5, 7.0)$ and for ten constant rest mass sequences with $M_0 \in (2.75, 3.75)$ for NL3 and $M_0 \in (1.75, 2.75)$ for SFHO. We found that there are relations between their physical properties that depend only weakly on the parameter \hat{A} . Examples of \hat{A} -independent relations that we found are shown in Figures 2 and 3, where we find that for NL3 EOS and SFHO EOS the rest mass and the angular momentum are related in a way which is practically independent of \hat{A} .

Since it is quite formidable to test every value of \hat{A} for every single one of the 13 different EOS in Table 1 (not only for the two we tested), we conjecture that the \hat{A} -insensitive relations found for the two representative EOS SFHO and NL3, will remain \hat{A} -insensitive also for the other tabulated EOS. This means that *universal (EOS-insensitive) relations valid for uniform rotation, should remain universal*

for differential rotation, if we can demonstrate that they are \hat{A} -insensitive for some representative EOS.

For uniformly rotating models, we checked universality of relations for all EOS by locating turning points of ten equispaced constant angular momentum sequences with angular momentum from 0.5 to 7.0. We chose this range because it covers all the allowed sequences for most EOS, as only the stiffest ones can reach values of angular momentum greater than 7.0 before encountering the mass-shedding limit in uniform rotation, or before entering a region in the parameter space where models have too small axis ratio to be considered realistic for binary neutron star merger remnants. We computed only constant angular momentum sequences, because the above range is suitable for all the EOS, whereas the allowed range for rest masses depends on the stiffness of the EOS so it would have required adjusting the range for each EOS.

First, for each EOS we found three relations involving the gravitational mass M , the rest mass M_0 , and the angular momentum J that are \hat{A} -insensitive with an error $\sigma_{\hat{A}}$ of 0.5 – 1.0 per cent. This means that if x is a physical quantity among the ones mentioned, and $f_{\hat{A}}$ one of the relations discovered, then:

$$\frac{|f_{\text{uni}}(x) - f_{\hat{A}}(x)|}{|f_{\text{uni}}(x)|} \leq 1\% \quad \forall \hat{A} \geq 0.5, \quad (11)$$

where f_{uni} is the relation evaluated with uniform rotation ($\hat{A} = +\infty$). The three \hat{A} -insensitive relations we found for each EOS are simple functions of the form:

$$M_0 = M_0(J), \quad (12a)$$

$$M_0 = M_0(M), \quad (12b)$$

$$M = M(J). \quad (12c)$$

For a fixed angular momentum J , the effect of decreasing \hat{A} is to lower the corresponding rest mass but to increase the gravitational mass. On the other hand, for a fixed rest mass M_0 , a reduction of \hat{A} produces an increase in the angular momentum and gravitational mass. While the strength of the effect produced by varying \hat{A} depends on the stiffness of the EOS, it always stays smaller than 1%.

We obtain EOS-independent universal relations by rescaling relations (12a), (12b) and (12c) using M^* and M_0^* as follows:

$$\frac{M_0}{M_0^*} = 1 + 0.51 \left(\frac{cJ}{GM_0^{*2}} \right)^2 - 0.28 \left(\frac{cJ}{GM_0^{*2}} \right)^4, \quad (13a)$$

$$\frac{M_0}{M_0^*} = 0.93 \frac{M}{M^*} + 0.07, \quad (13b)$$

$$\frac{M}{M^*} = 1 + 0.29 \left(\frac{cJ}{GM^{*2}} \right)^2 - 0.10 \left(\frac{cJ}{GM^{*2}} \right)^4. \quad (13c)$$

As an example, we show (13c) in Figure 4 (black solid line). Every colour is a different equation of state and the gray shade is the 1.2% error bar inside which every point lies. Similar maximum relative errors (1.2% and 1.6%) hold for the other two universal relations (13a) and (13b), which are shown in Figures 5 and 6.

Notice that, inverting relation (13a) we also find a universal relation for the Kerr parameter $a := cJ/GM^2$ of the form:

$$a = a \left(\frac{M}{M^*} \right) \quad (14)$$

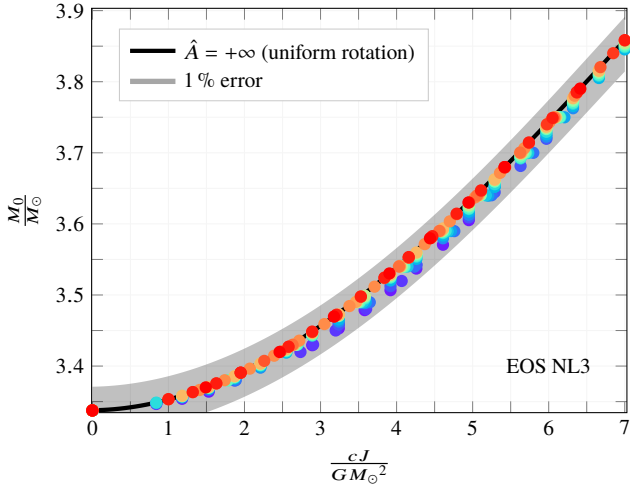


Figure 2. \hat{A} -independent relation between rest mass and angular momentum for the EOS NL3. This plot is obtained by finding the turning points for ten constant rest mass and angular momentum sequences with \hat{A} between 0.5 and 2.0 and with values in the range $\{2.5, 3.0, 4.0\}$. Different colours represent different rotation parameters. Sequences with the same angular momentum (but different \hat{A}) divert vertically, whereas sequences with the same rest mass divert horizontal horizontally. The effect of decreasing \hat{A} to lower the corresponding rest mass, and to increase the angular momentum. Overall this change is less than 1%, therefore all the sampled points lie on the same curve within this error bar.

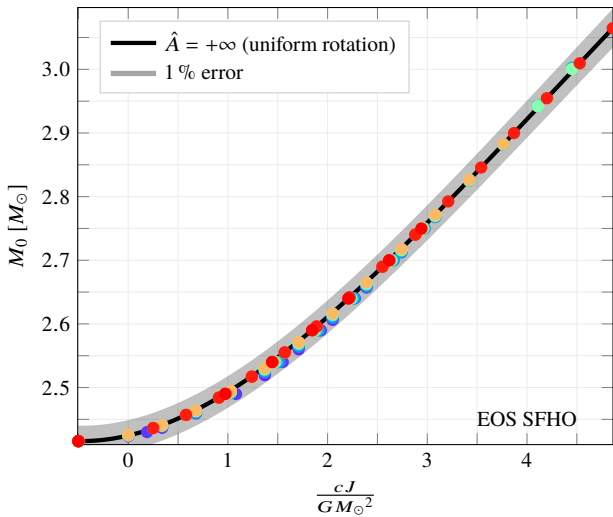


Figure 3. Same as Fig. 2, but for EOS SFHO.

Combining the maximum relative error of the universal relations for uniform rotation with the maximum deviation due to differential rotation, we find that relations (13a) and (13b) should be universal for differentially rotating stars with a maximum relative error of about 2% (more specifically, for the range of astrophysically relevant values of \hat{A} we considered with the one-parameter law (5)).

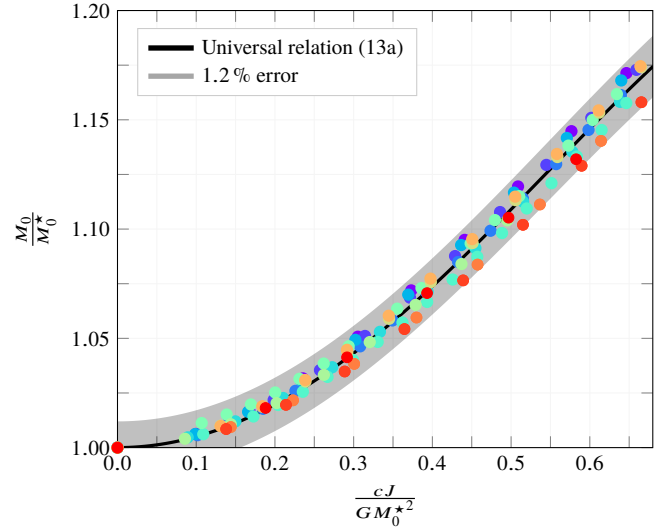


Figure 4. Universal (EOS-independent) relation between scaled rest mass and scaled angular momentum. The turning points for constant angular momentum sequences for uniformly rotating stars and different EOS, are shown with a different colour. All the points lie within a 1.2% error bar.

3.1.2 Three-parameter rotation law

In Section 3.1.1 we used the one-parameter rotation law (5) (and with uniform rotation as a special case). For the three-parameter rotation law (7) we computed the turning points for a finite subset of values of \hat{A}_1, \hat{A}_2 and β . We combined in all the possible ways the values of $\hat{A}_{1(2)} \in \{0.5, 1.0, 2.5\}$ and of $\beta \in \{0.6, 0.8\}$, computing for each case eight sequences of constant angular momentum $J \in (0.5, 7.0)$ and eight sequences of constant rest mass $M_0 \in (1.75, 2.75)$ for the EOS NL3 and $M_0 \in (1.75, 2.75)$ for the EOS SFHO.

In all cases studied, we confirmed that the universal relations presented in Section 3.1.1 still hold. This indicates that these relations may retain universality for even more general rotation laws than (5) or (7), at least for quasi-spherical models considered here.

3.1.3 Polytropic EOS

We performed the same analysis of the Section 3.1.1 on the two polytropic equations of state rotating with the one-parameter law finding agreement with the previously presented relations. Moreover, polytropes showed clearly how the stiffness of the equation of state affects the universal relations.

First, we noticed that for the $n = 1.0$ polytrope the relation between rest mass and gravitational mass (depicted in Figure 7) is especially accurate, with error smaller than 0.3 per cent, but somewhat larger for the $n = 0.5$ polytrope. On the other hand, for the polytrope with $n = 0.5$ the relation between gravitational mass and angular momentum has accuracy of 0.3%, but it has $\sim 2\%$ error in the case of $n = 1.0$. In addition, the relation satisfied within $\sim 2\%$ shows clearly how the small dependence on \hat{A} affects the physical quantities of the turning-point models (see inset of Figure 7),

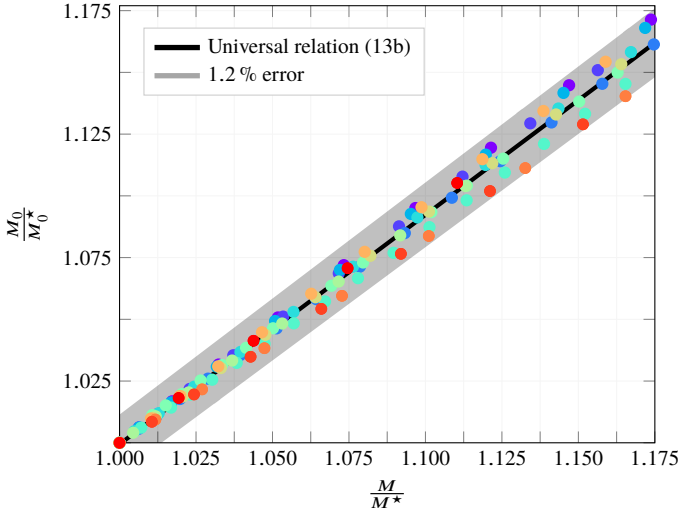


Figure 5. Universal (EOS-independent) relation between scaled rest mass and scaled gravitational mass. The turning points for constant angular momentum sequences for uniformly rotating stars and different EOS, are shown with a different colour. All the points lie within a 1.2% error bar.

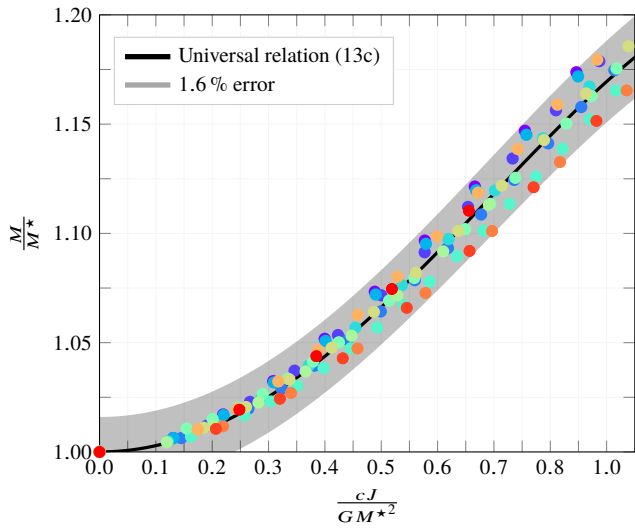


Figure 6. Universal (EOS-independent) relation between scaled gravitational mass and scaled angular momentum. The turning points for constant angular momentum sequences for uniformly rotating stars and different EOS, are shown with a different colour. All the points are within 1.6% error bars.

which is similar to the effect described in Section 3.1.1 for tabulated EOS.

Having verified that there are some \hat{A} -independent relations we checked whether polytropes satisfied Equations (13a), (13b) and (13c). We found agreement, as shown in Figure 8.

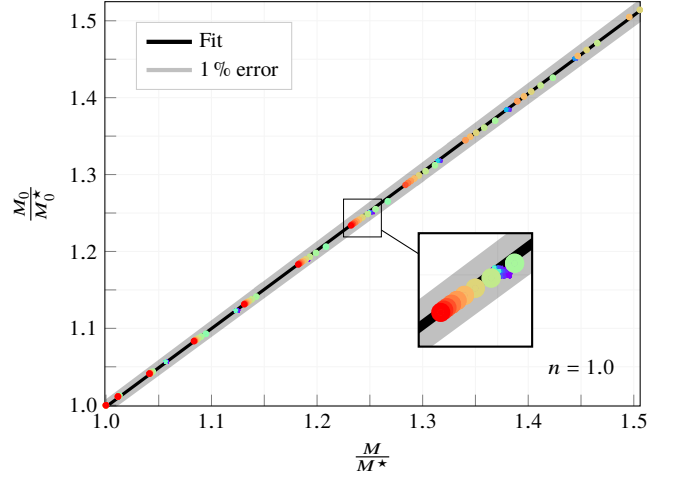


Figure 7. \hat{A} -independent relation between scaled rest mass and scaled gravitational mass for a polytrope with index $n = 1.0$. The relation is satisfied within a relative error of 1%. Nearby circles represent a sequence with the same angular momentum but different values of \hat{A} : decreasing \hat{A} increases both the rest mass and the gravitational mass in a way that the linear relation is satisfied. The accuracy of this relation is 0.3%, whereas it is 1% in the case of the $n = 0.5$ polytrope.

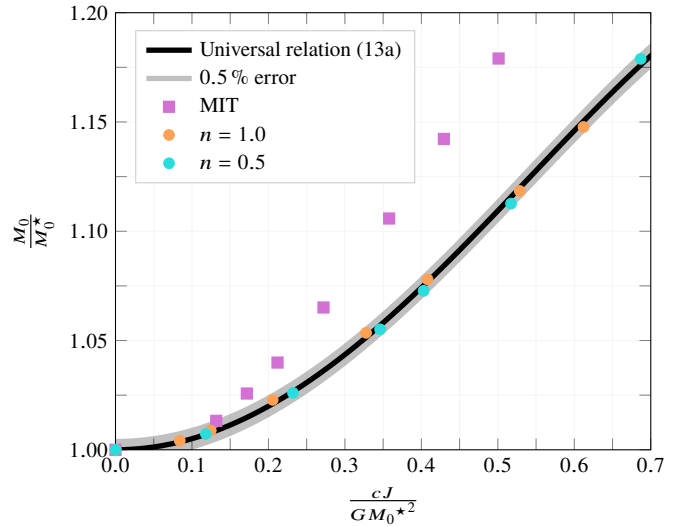


Figure 8. Scaled rest mass vs. scaled angular momentum relation for polytropic $n = 0.5$ and $n = 1.0$ and strange star (MIT) EOS. The polytropic EOSs satisfy the universal relation constructed with the tabulated EOSs with high accuracy. In contrast, the strange star EOS deviates significantly from the universal relation.

3.1.4 Strange star EOS

Testing the relations with uniformly rotating strange stars produced a counterexample: the turning points of constant angular momentum sequences have a significantly different relation between rest mass and angular momentum than for tabulated EOS (or polytropes). This situation is shown in Figure 8. A fit to the data obtained with the strange star

EOS is

$$\frac{M_0}{M_0^*} \left(\frac{cJ}{GM_0^{*2}} \right) = 1 + 0.87 \left(\frac{cJ}{GM_0^{*2}} \right)^2 - 0.60 \left(\frac{cJ}{GM_0^{*2}} \right)^4. \quad (15)$$

Equation (15) and Equation (13a) are compatible only in the limit of slow rotation, while for $J/(M_0^*)^2 = 0.9$ the discrepancy is already 15%.

4 SUMMARY

Using the general-relativistic code RNS we investigated the properties of turning points of equilibrium sequences of differentially rotating stars, using a variety of EOS. Our interest is justified by the Friedman, Iper and Sorkin's method that allows us to estimate the stability properties of rotating stars without performing full dynamical simulations.

Sampling the parameter space of the stellar models rotating with a one-parameter law for differential rotation, we found that the properly scaled gravitational mass, rest mass and angular momentum of the turning points satisfy universal relations that are independent of the EOS and the degree of differential rotation to high accuracy. A counterexample are strange stars, which do not obey the same universal relations as tabulated or polytropic EOS. We verified that the relations still hold for a more general, three-parameter rotation law, indicating that they might hold for an even larger class of rotation laws.

Future work could extend our analysis to realistic rotation laws extracted from dynamical simulations and the finite-temperature, pseudobarotropic models.

ACKNOWLEDGEMENTS

Computations were performed on the LCM cluster by INFN in Milan (Italy). We thank Matthias Hempel for providing EoS tables. A.B. acknowledges support by the Klaus Tschira Foundation.

REFERENCES

Abadie J., et al., 2010, *Class. Quantum Grav.* 27, 173001
 Accadia T., et al., 2011, *Class. Quantum Grav.* 28, 114002
 Alcock C., Farhi E., Olinto A., 1986, *ApJ*, 310, 261
 Ansorg M., Gondek-Rosińska D., Villain L., 2009, *MNRAS*, 396, 2359
 Antoniadis J., et al., 2013, *Science*, 340
 Arnett W. D., Bowers R. L., 1977, *ApJS*, 33, 415
 Baiotti L., Rezzolla L., 2017, *Reports on Progress in Physics*, 80, 096901
 Baiotti L., Giacomazzo B., Rezzolla L., 2008, *Phys. Rev.*, D78, 084033
 Banik S., Hempel M., Bandyopadhyay D., 2014, *ApJS*, 214, 22
 Bardeen J. M., Wagoner R. V., 1971, *ApJ*, 167, 359
 Baumgarte T. W., Shapiro S. L., Shibata M., 2000, *ApJ*, 528, L29
 Bauswein A., Stergioulas N., 2017, preprint, ([arXiv:1702.02567](https://arxiv.org/abs/1702.02567))
 Bauswein A., Baumgarte T. W., Janka H.-T., 2013, *Phys. Rev. Lett.*, 111, 131101
 Breu C., Rezzolla L., 2016, *MNRAS*, 459, 646
 Cook G. B., Shapiro S. L., Teukolsky S. A., 1994, *ApJ*, 422, 227

Demorest P. B., Pennucci T., Ransom S. M., Roberts M. S. E., Hessels J. W. T., 2010, *Nature*, 467, 1081
 Faber J. A., Rasio F. A., 2012, *Living Reviews in Relativity*, 15, 8
 Friedman J. L., Iper J. R., 1987, *ApJ*, 314, 594
 Friedman J. L., Stergioulas N., 2013, *Rotating Relativistic Stars*. Cambridge University Press
 Friedman J. L., Iper J. R., Sorkin R. D., 1988, *ApJ*, 325, 722
 Gondek-Rosińska D., Kowalska I., Villain L., Ansorg M., Kucaba M., 2017, *ApJ*, 837, 58
 Haensel P., Zdunik J. L., Schaefer R., 1986, *A&A*, 160, 121
 Hanauske M., Takami K., Bovard L., Rezzolla L., Font J. A., Galeazzi F., Stöcker H., 2017, *Phys. Rev. D*, 96, 043004
 Hempel M., 2017, EOS Tables, <http://www.phys-merger.physik.unibas.ch/~hempel/eos.html>
 Hempel M., Schaffner-Bielich J., 2010, *Nuclear Phys. A*, 837, 210
 Hotokezaka K., Kyutoku K., Okawa H., Shibata M., Kiuchi K., 2011, *Phys. Rev. D*, 83, 124008
 Kaplan J. D., Ott C. D., O'Connor E. P., Kiuchi K., Roberts L., Duez M., 2014, *ApJ*, 790, 19
 Kastaun W., Ciolfi R., Giacomazzo B., 2016, *Phys. Rev. D*, 94, 044060
 Komatsu H., Eriguchi Y., Hachisu I., 1989a, *MNRAS*, 237, 355
 Komatsu H., Eriguchi Y., Hachisu I., 1989b, *MNRAS*, 239, 153
 Lalazissis G. A., König J., Ring P., 1997, *Phys. Rev. C*, 55, 540
 Lattimer J. M., Swesty F. D., 1991, *Nuclear Phys. A*, 535, 331
 Lenka S. S., Char P., Banik S., 2017, preprint, ([arXiv:1704.07113](https://arxiv.org/abs/1704.07113))
 Lyford N. D., Baumgarte T. W., Shapiro S. L., 2003, *ApJ*, 583, 410
 Morrison I. A., Baumgarte T. W., Shapiro S. L., 2004, *ApJ*, 610, 941
 Nozawa T., Stergioulas N., Gourgoulhon E., Eriguchi Y., 1998, *A&AS*, 132, 431
 Oppenheimer J. R., Volkoff G. M., 1939, *Phys. Rev.*, 55, 374
 Paschalidis V., Stergioulas N., 2016, preprint, ([arXiv:1612.03050](https://arxiv.org/abs/1612.03050))
 Roca-Maza X., Piekarewicz J., 2008, *Phys. Rev. C*, 78, 025807
 Shibata M., 2005, *Phys. Rev. Lett.*, 94, 201101
 Shibata M., Taniguchi K., 2006, *Phys. Rev. D*, 73, 064027
 Shibata M., Taniguchi K., Uryū K., 2005, *Phys. Rev. D*, 71, 084021
 Somiya K., 2012, *Class. Quantum Grav.* 29, 124007
 Steiner A. W., Hempel M., Fischer T., 2013, *ApJ*, 774, 17
 Stergioulas N., 1999, Rapidly rotating neutron star, <https://www.gravity.phys.uwm.edu/rns>
 Stergioulas N., Friedman J. L., 1995, *ApJ*, 444, 306
 Stergioulas N., Apostolatos T. A., Font J. A., 2004, *MNRAS*, 352, 1089
 Sugahara Y., Toki H., 1994, *Nuclear Phys. A*, 579, 557
 Takami K., Rezzolla L., Yoshida S., 2011, *MNRAS*, 416, L1
 Tolman R. C., 1934, *Proc. Natl. Acad. Sci.*, 20, 169
 Typel S., Röpke G., Klähn T., Blaschke D., Wolter H. H., 2010, *Phys. Rev. C*, 81, 015803
 Wiringa R. B., Fiks V., Fabrocini A., 1988, *Phys. Rev.*, C38, 1010
 Witten E., 1984, *Phys. Rev. D*, 30, 272
 Zdunik J. L., 2000, *A&A*, 359, 311

This paper has been typeset from a $\text{\TeX}/\text{\LaTeX}$ file prepared by the author.